

REGULAR PAPER • OPEN ACCESS

# Energetics and bistable morphologies of transition-metal dichalcogenide nanoscrolls

To cite this article: Yanlin Gao *et al* 2026 *Jpn. J. Appl. Phys.* **65** 055001

View the [article online](#) for updates and enhancements.

## You may also like

- [Twists and turns: stacking and structure-dependent optical response in MoS<sub>2</sub> nanoscrolls](#)  
Sagnik Chatterjee, Tamaghna Chowdhury, Pablo Díaz-Núñez *et al.*
- [Tunable bending stiffness of MoSe<sub>2</sub>/WSe<sub>2</sub> heterobilayers from flexural wrinkling](#)  
Yufeng Guo, Jiapeng Qiu and Wanlin Guo
- [Effect of misfit strain on the buckling of graphene/MoS<sub>2</sub> van der Waals heterostructures](#)  
Run-Sen Zhang and Jin-Wu Jiang



# Energetics and bistable morphologies of transition-metal dichalcogenide nanoscrolls

Yanlin Gao<sup>1,2\*</sup> , Mina Maruyama<sup>1,2\*</sup> , Yasumitsu Miyata<sup>3\*</sup> , and Susumu Okada<sup>1,2\*</sup>

<sup>1</sup>Department of Physics, Graduate School of Science and Technology, University of Tsukuba, 1-1-1 Tennodai, Tsukuba, Ibaraki 305-8571, Japan

<sup>2</sup>Tsukuba Institute for Advanced Research (TIAR), University of Tsukuba, 1-1-1 Tennodai, Tsukuba, Ibaraki 305-8577, Japan

<sup>3</sup>Research Center for Materials Nanoarchitectonics, National Institute for Materials Science, Tsukuba 305-0044, Japan

\*E-mail: [ylgao@comas-tsukuba.jp](mailto:ylgao@comas-tsukuba.jp); [mmaruyama@comas-tsukuba.jp](mailto:mmaruyama@comas-tsukuba.jp); [MIYATA.Yasumitsu@nims.go.jp](mailto:MIYATA.Yasumitsu@nims.go.jp); [sokada@comas-tsukuba.jp](mailto:sokada@comas-tsukuba.jp)

Received December 11, 2025; revised January 18, 2026; accepted February 4, 2026; published online March 2, 2026

Using a continuous elastic model combined with intershell van der Waals interaction, we investigated the energetics of nanoscrolls formed from the transition-metal dichalcogenides (TMDs) MoS<sub>2</sub>, MoSe<sub>2</sub>, WS<sub>2</sub>, WSe<sub>2</sub>, MoSSe, and WSSe. We found that, for TMD nanoscrolls with short rolled lengths, the strain effect competes with van der Waals effects to determine the geometries of the nanoscrolls. By contrast, for long rolled lengths, van der Waals effects dominate, leading to a high stability of the scrolled conformation for all TMDs. For Janus TMD nanoscrolls with short rolled length, the combination of curvature induced by the intrinsic strain and van der Waals interactions leads to bistable morphologies, characterized by scroll and arch conformations. These conformations can be switched by external conditions. © 2026 The Author(s). Published on behalf of The Japan Society of Applied Physics by IOP Publishing Ltd

## 1. Introduction

The tight in-plane covalent bonding network and electronically saturated surfaces of atomic-layer materials make them attractive building blocks for various compounds, in which they can be freely stacked without the constraints imposed by chemical bonds in conventional condensed matter.<sup>1–4)</sup> Such complexes have unique physical properties, which exceed those of the superposition of the constituent atomic layers because of their substantial wavefunction overlap, even though they are only weakly bound.<sup>3,4)</sup> In addition, atomic-layer materials can exhibit morphological variation depending on the boundary conditions imposed on them. Nanotubes,<sup>5–12)</sup> nanoscrolls,<sup>13–19)</sup> and nanoribbons<sup>20,21)</sup> are representative examples of such nanomorphologies derived from atomic-layer materials by imposing open and periodic one-dimensional boundary conditions along the circumference. These boundary conditions lead to unconventional physical properties in the morphological derivatives, depending on their size and shape. Carbon nanotubes are either metals or semiconductors, depending on the atomic arrangement along their circumference, which corresponds to the quantization condition.<sup>6)</sup> Graphene nanoribbons with zigzag edges possess a peculiar edge-localized state arising from quantum interference of wavefunctions around edge atomic sites.<sup>20,21)</sup>

Among the one-dimensional morphologies of atomic-layer materials, nanoscrolls have a unique structure, which is characterized by a continuously varying curvature from the innermost to the outermost shells, as well as intershell interactions and edge effects.<sup>13–18,22–26)</sup> In particular, the curvature effect determines the electronic properties of nanoscrolls, because the electronic structures of atomic-layer materials are sensitive to curvature.<sup>27–31)</sup> Graphene nanoscrolls and Janus WSSe nanoscrolls exhibit remarkable stability and a unique electronic structure along their circumference.<sup>25,26)</sup> For example, WSSe nanoscrolls are semiconductors that show band bending along the scroll, resulting in type-II band-edge alignment between the inner

and outer shells of the scroll.<sup>26)</sup> This band-edge bending is attributed to the radial dipole moment arising from the curvature and asymmetric chalcogen arrangement across the shell. The electronic structure of graphene nanoscrolls also exhibits a strong position dependence that is sensitive to the nanoscroll shape. This dependence is due to electrostatic potential modulation and intershell orbital hybridization exerted by the multishell structure.<sup>25)</sup> The aforementioned theoretical works imply that the electronic structure of nanoscrolls can be tuned by controlling their conformation and constituent elements.

Although the energetics and electronic properties of nanoscrolls with small diameters have been investigated, little is known about nanoscrolls with large diameters and multiple intershell stackings.<sup>23–26)</sup> In this work, we aim to investigate the energetics of transition-metal dichalcogenide (TMD) nanoscrolls for providing qualitative and comprehensive knowledge about scroll geometries using a continuous elastic model combined with intershell van der Waals interactions, in which all parameters were determined using density functional theory (DFT). We considered MoS<sub>2</sub>, MoSe<sub>2</sub>, WS<sub>2</sub>, and WSe<sub>2</sub> nanoscrolls for conventional TMDs and MoSSe and WSSe nanoscrolls as Janus TMDs, whose rolled length ( $L$ ) is varied, ranging from 10 to 100 nm. Our analyses demonstrated that strain and van der Waals effects compete to determine the geometries of TMD nanoscrolls for the short rolled length, while van der Waals effects dominate for the long rolled length. For Janus TMDs with the short rolled length, the combination of curvature induced by intrinsic strain and van der Waals interactions leads to bistable morphologies, characterized by nanoscroll and nanoarch structures.

## 2. Calculation methods

To construct the elastic model that describes the curvature effect of TMDs, we investigated the total energy of TMD nanotubes using DFT<sup>32,33)</sup> implemented in the program package Simulation Tool for Atom TEchnology.<sup>34,35)</sup> We



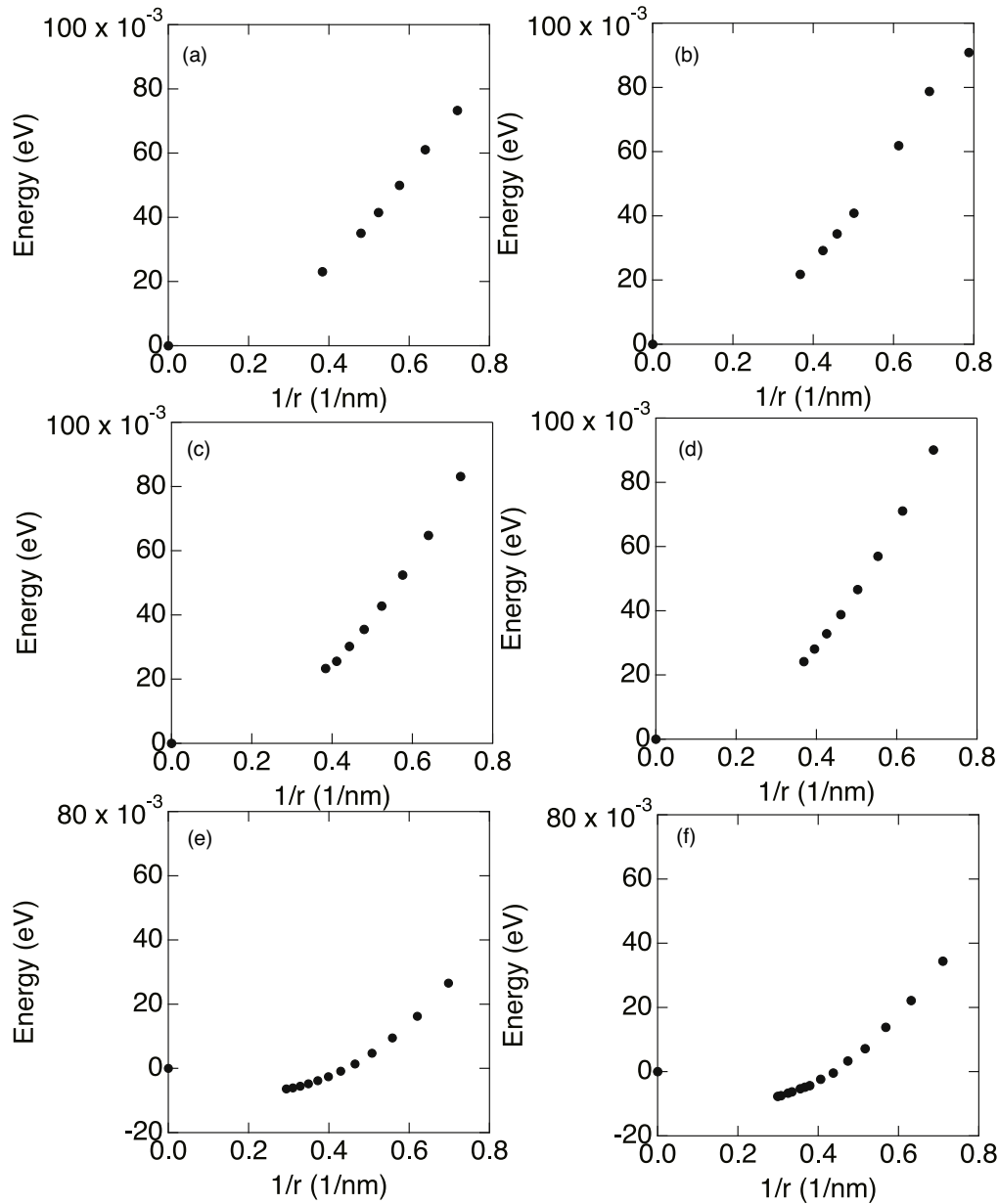


**Fig. 1.** Total energy per atom of MoS<sub>2</sub>, MoSe<sub>2</sub>, WS<sub>2</sub>, WSe<sub>2</sub>, MoSSe, and WSSe nanotubes as a function of the inverse of their radius,  $r$ . The energies were measured relative to those of the corresponding isolated sheets.

considered armchair MoS<sub>2</sub>, MoSe<sub>2</sub>, WS<sub>2</sub>, WSe<sub>2</sub>, MoSSe, and WSSe nanotubes. The exchange-correlation energy among the interacting electrons was expressed using the generalized gradient approximation (GGA) with the functional form of the Perdew–Burke–Ernzerhof functional.<sup>36,37)</sup> Ultrasoft pseudopotentials generated using the Vanderbilt scheme were used to describe electron–ion interactions.<sup>38)</sup> The valence wavefunctions and deficit charge density were expanded in terms of the plane-wave basis set with cutoff energies of 25 and 225 Ry, respectively. Integration over the one-dimensional Brillouin zone was carried out using equidistant  $k$ -point sampling in which 5  $k$ -points were taken along the TMD nanotube axis. This allowed us to conduct calculations on TMD nanotubes with diameters up to approximately 5 nm. The atomic structures of these nanotubes were optimized until the force acting on each atom was less than 5 mRy Å<sup>-1</sup>. The lattice parameter along the tube axis was fixed to the optimized lateral lattice parameters of the isolated monolayer TMD sheets.

Figure 1 shows the total energies per atom of MoS<sub>2</sub>, MoSe<sub>2</sub>, WS<sub>2</sub>, WSe<sub>2</sub>, MoSSe, and WSSe nanotubes with respect to the corresponding isolated sheets as a function of the inverse of the radius. The total energy of the tubular materials is inversely proportional to the square of the radius. Thus, the energies were fitted using the quadruple polynomial of the inverse of the radius:

$$\varepsilon_s(r) = \frac{D}{r^2} + \frac{B}{r} \quad (1)$$

[where  $D$  and  $B$  are coefficients depending on the tube species. Evaluated coefficients are listed in Table I. Equation (1) corresponds to the energy cost to bend the TMD with curvature radius  $r$ . TMD nanoscrolls are modeled by the contentious elastic model shown in Fig. 2 in which the structure is characterized by the innermost shell radius  $r_0$ , TMD thickness  $\Delta$ , intershell spacing  $d$ , and scroll angle  $\theta$  which assign the particular position on nanoscroll. The local curvature radius  $r(\theta)$  of the nanoscroll is defined as

**Table I.** The coefficients  $D$  and  $B$  of the quadruple polynomial fitted to the total energies of MoS<sub>2</sub>, MoSe<sub>2</sub>, WS<sub>2</sub>, WSe<sub>2</sub>, MoSSe, and WSSe nanotubes.

	MoS <sub>2</sub>	MoSe <sub>2</sub>	WS <sub>2</sub>	WSe <sub>2</sub>	MoSSe	WSSe
$D$ (eV nm <sup>2</sup> )	0.1393	0.1663	0.1586	0.2014	0.1462	0.1790
$B$ (eV nm)	—	—	—	—	−0.0648	−0.0789

$$r(\theta) = r_0 + \frac{\Delta + d}{2\pi}\theta. \quad (2)$$

In this work, we assumed  $\Delta = 0.3$  nm and  $d = 0.3$  nm, which are approximate values for TMD monolayers and bilayers.<sup>39)</sup> Using a typical interlayer van der Waals interaction  $\varepsilon_v = 0.02$  eV/atom under  $d = 0.3$  nm, the total energy of the TMD nanoscrolls was evaluated as

$$E(L, r_0) = \int_0^L dl \{\varepsilon_s(r) + \varepsilon_v\} \quad (3)$$

where  $L$  is the rolled length of TMD nanoscrolls corresponding to the width of flat TMD nanoribbons. Using Eq. (2), the total energy of the TMD nanoscrolls can be expressed as

$$E(L, r_0) = \int_0^\alpha d\theta \left\{ \frac{D}{r_0 + \frac{\Delta + d}{2\pi}\theta} + \varepsilon_v \left( r_0 + \frac{\Delta + d}{2\pi}\theta \right) \right\} \quad (4)$$

where the angle  $\alpha$  is the total rotational angle corresponding to the rolled length  $L (= \int_0^\alpha d\theta r)$ .

### 3. Results and discussion

#### 3.1. MX<sub>2</sub> (M = Mo, W and X = S, Se) nanoscrolls

Figure 3 shows the total energy of MoS<sub>2</sub>, MoSe<sub>2</sub>, WS<sub>2</sub>, and WSe<sub>2</sub> nanoscrolls as a function of the rolled length  $L$  and the innermost radius  $r_0$ . Conventional TMDs prefer a flat conformation in their isolated form because of the symmetric chalcogen arrangement around the transition-metal atom layer. The total energy increases with increasing curvature, which corresponds to the increase of strain, irrespective of the ribbon width or rolled length  $L$ . For ribbons with a narrow width or scrolls with short rolled length  $L < 20$  nm, the total energy increases monotonically with increasing curvature, even though they possess a scroll conformation. In this region, the energy gain by the intershell van der Waals interaction is insufficient to overcome the energy cost associated with the mechanical strain induced by the large curvature. Upon further increasing the rolled length  $L$  to approximately 20 nm, a cusp emerges, which turns into a local minimum at approximately  $r_0 = 2$  nm. For rolled lengths  $L = 45.7, 47.5, 44.6$ , and  $41.8$  nm for MoS<sub>2</sub>, MoSe<sub>2</sub>, WS<sub>2</sub>, and WSe<sub>2</sub>, respectively, the energy of the scrolled structure is lower than that of their flat conformation, indicating that the scrolled conformation is the possible ground state for the one-dimensional TMD nanostructure owing to the substantial van der Waals inter-shell interaction. The evaluated innermost shell radii  $r_0$  at the critical rolled length  $L$  were 4.4, 4.5, 4.2, and 3.9 nm for MoS<sub>2</sub>, MoSe<sub>2</sub>, WS<sub>2</sub>, and WSe<sub>2</sub>, respectively. The innermost radii depend on the rolled length  $L$ . The radii were

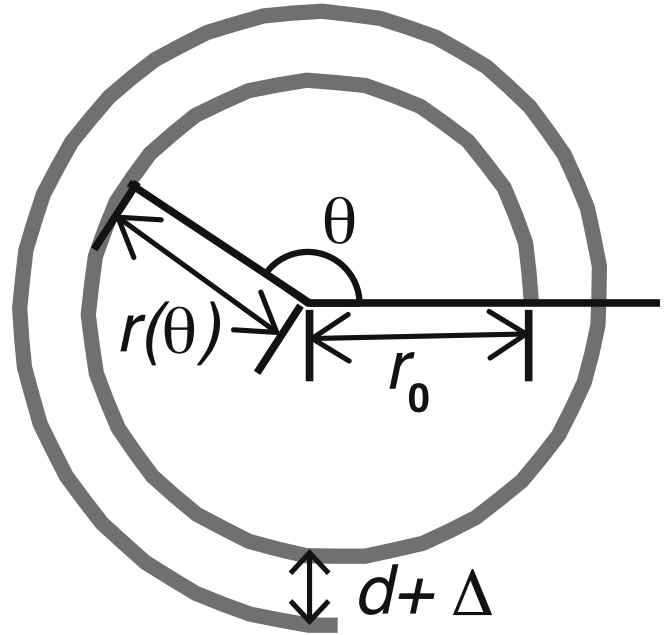


**Fig. 2.** A structural model of the TMD nanoscroll, where the nanoscroll is denoted by a gray curve. The  $r_0$  is the innermost shell radius of the scroll, and  $\theta$  is the scroll angle specifying the position on the scroll. Each shell is separated by the sum of the intershell spacing  $d$  and the TMD thickness  $\Delta$ .

5.4, 5.6, 5.3, and 5.0 nm for MoS<sub>2</sub>, MoSe<sub>2</sub>, WS<sub>2</sub>, and WSe<sub>2</sub>, respectively, for the rolled length  $L = 100$  nm. We attribute the increase in the innermost-shell radius  $r_0$  to increased shell overlap at long rolled length, leading to a substantial energy gain from van der Waals interactions. Thus, the delicate balance between the strain energy and the inter-shell van der Waals interaction determines the conformation of the one-dimensional nanostructure of TMDs under appropriate external conditions. We conclude that the nanoscrolls represent their possible ground-state conformation of one-dimensional structures derived from atomic-layer materials with sufficient intershell overlap. It is plausible that the multiply-folded conformation is another possible ground-state configuration for one-dimensional structures derived from atomic-layer materials with sufficient intershell overlap.<sup>40)</sup>

The geometric structure of MoS<sub>2</sub> nanoscrolls is depicted in Fig. 4. The TMD has a characteristic morphology corresponding to different energy landscapes. Under the local minimum, the TMD has a scrolled structure with substantial intershell overlap [Fig. 4(a)]. By contrast, at the energy barrier, it assumes a scroll conformation with small shell overlap corresponding [Fig. 4(b)]. Furthermore, the total energy of TMD nanoscrolls substantially decreases with increasing number of shells for long rolled length  $L$  [Fig. 4(c)]. Thus, the energetics and conformations of TMD nanoscrolls are determined by the delicate balance between the strain energy derived from curvature and the intershell van der Waals interaction.

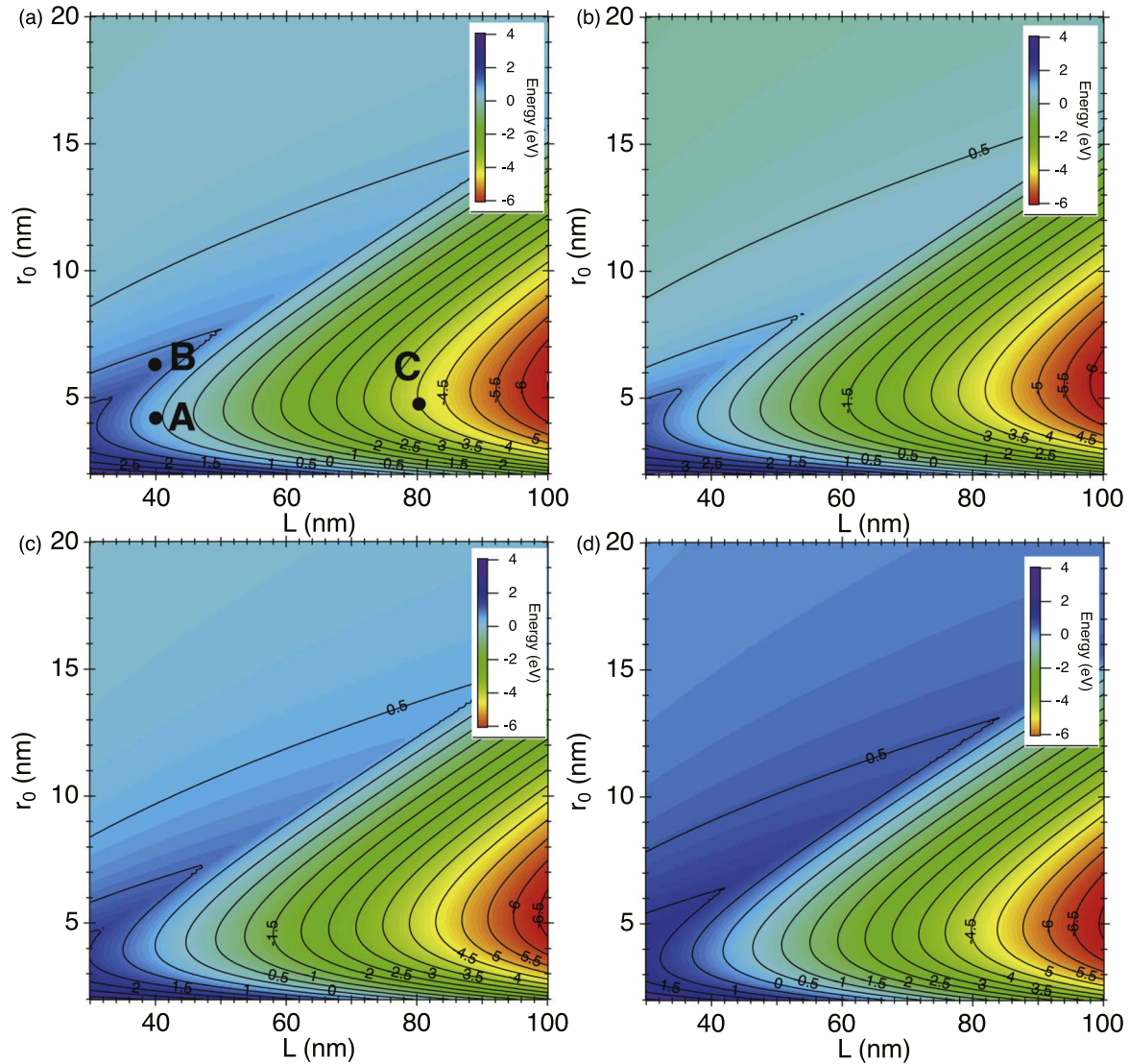


**Fig. 3.** Contour plots of the total energy per nanoscroll unit of (a) MoS<sub>2</sub>, (b) MoSe<sub>2</sub>, (c) WS<sub>2</sub>, and (d) WSe<sub>2</sub> nanoscrolls as a function of the rolled length  $L$  and the innermost radius  $r_0$  of TMD nanoscrolls. The energy was measured from the flat conformation for each rolled length.

### 3.2. Janus MSSe ( $M = \text{Mo, W}$ ) nanoscrolls

Figure 5 shows the total energy of MoSSe and WSSe nanoscrolls as a function of the rolled length  $L$  and the innermost radius  $r_0$ . The stable conformations of MoSSe and WSSe ribbons and sheets exhibit curvature because of the intrinsic tensile and compressive strains derived from the structural asymmetry of the chalcogene layers. The curvature radius in the stable conformation was calculated to be 4.4 nm for MoSSe and WSSe, irrespective of the rolled length. A new structure in the energy landscape appears near the innermost radius  $r_0 = 2$  nm at the rolled lengths  $L = 15$  nm and 16 nm for MoSSe and WSSe, respectively, and a minimum appears near  $r_0 = 2.2$  nm, upon further increasing the rolled length  $L$ . The minima near  $r_0 = 2$  nm are metastable up to the rolled length  $L = 20$  nm and are deeper than those corresponding to the intrinsic curvature. These minima correspond to the scrolled conformation of the Janus TMD, where van der Waals interactions are comparable to or dominate the strain energy, thereby stabilizing the scrolled conformation. In particular, wide Janus TMD sheets prefer a scrolled conformation, despite the large energy cost associated with the large curvature in their innermost shell. We

note that Janus TMD nanoscrolls with the rolled length  $L$  from 16 to 25 nm exhibit bistability corresponding to scrolled and arch conformations, which can be controlled by adjusting the external conditions.

Finally, we discuss the conformations of bistable phases of one-dimensional Janus TMDs. As described above, Janus TMDs with a moderate rolled length  $L$  from 15 to 40 nm exhibit bistability in their energy landscape, with two distinct local minima. Figure 6 shows the geometric structures of a Janus MoSSe nanoscroll [Fig. 6(a)] and nanoarch [Fig. 6(b)] with the rolled length  $L = 25$  nm, which corresponds to local minima at  $r_0 = 2$  and 4 nm, respectively. In the nanoscroll, the large curvature increases the strain energy, whereas the intershell overlap leads to an energy gain from van der Waals interactions, which are dominant in determining the scroll conformation. By contrast, in the nanoarch, the moderate curvature with a radius of 4 nm releases the intrinsic tensile and compressive strains in the Janus MoSSe, stabilizing the arch conformation. The energy barrier between these two conformations is about 0.25 eV per scroll unit and depends on the scroll and arch lengths (Fig. 7). Furthermore, the relative stability of the two conformations is sensitive to the

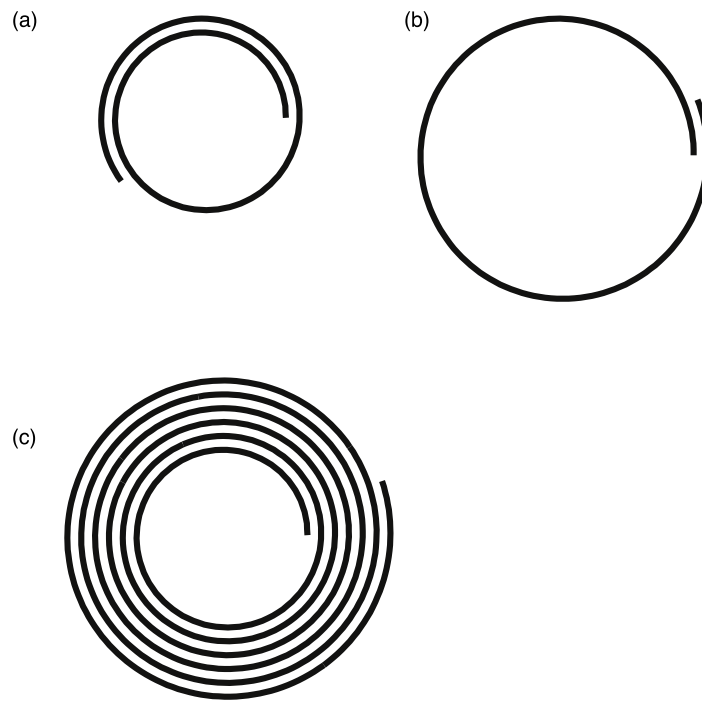


**Fig. 4.** Cross-sectional shape of MoS<sub>2</sub> with: (a)  $r_0 = 4$  nm and  $L = 40$  nm at position A in Figs. 2(a), 2(b)  $r_0 = 6$  nm and  $L = 40$  nm at position B in Fig. 2(a), and 2(c)  $r_0 = 4.5$  nm and  $L = 80$  nm at position C in Fig. 2(a). For simplicity, the atomic positions of Mo atoms are shown.

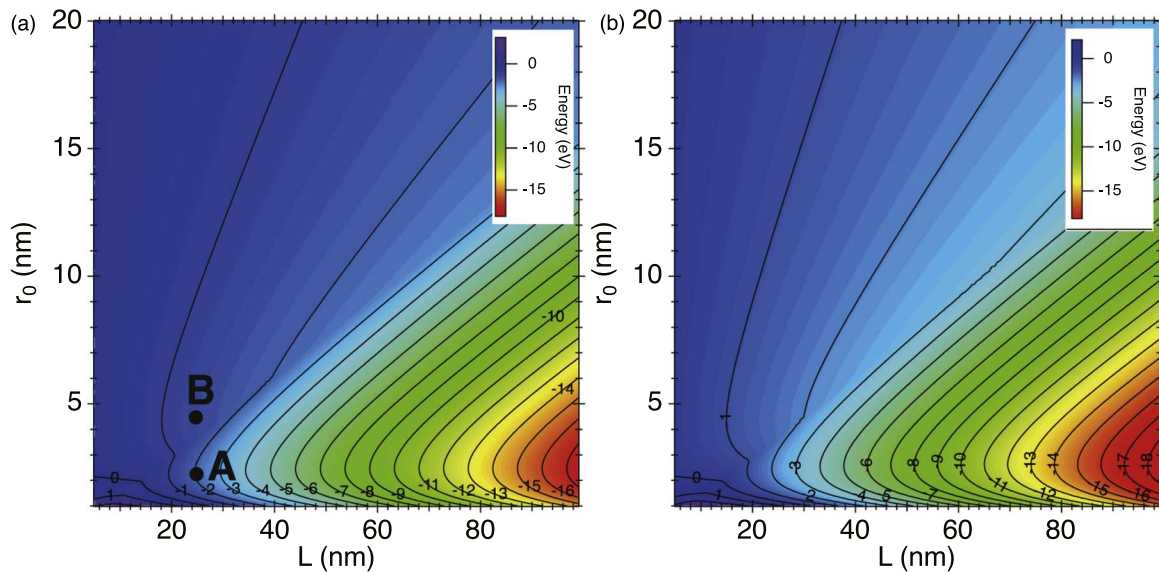


**Fig. 5.** Contour plots of the total energy per nanoscroll unit of (a) MoS<sub>2</sub> and (b) WSe<sub>2</sub> nanoscrolls as a function of the rolled length  $L$  and the innermost radius  $r_0$ . The energy is measured from their flat conformation at each rolled length.

rolled length  $L$  (Fig. 7): the nanoarch is more stable than the nanoscroll for short rolled length  $L$ , whereas the nanoscroll is more stable for long rolled length  $L$ . Thus, a structural phase transition is expected to occur between the two conformations under appropriate external conditions, enabling Janus TMD nanoscrolls and nanoarchs to serve as functional units for mechanical switching in nanodevices.

#### 4. Conclusions

We investigated the energetics of TMD nanoscrolls using a continuous elastic model combined with inter-shell van der Waals interactions, in which all parameters were determined using DFT. The strain energy as a function of the curvature radius was evaluated from total energy calculations on the armchair MoS<sub>2</sub>, MoSe<sub>2</sub>, WS<sub>2</sub>, WSe<sub>2</sub>, MoSSe, and WSeSe

nanotubes using DFT with GGA. The van der Waals interaction was set to a representative value of 0.02 eV/atom at the optimum interlayer spacing of TMD bilayers. We calculated the total energies of MoS<sub>2</sub>, MoSe<sub>2</sub>, WS<sub>2</sub>, WSe<sub>2</sub>, MoSSe, and WSeSe nanoscrolls for rolled lengths from 10 to 100 nm and for different innermost shell radii. Our calculations demonstrated that for short rolled lengths, strain and van der Waals effects compete to determine the nanoscroll geometry, whereas for long rolled lengths, van der Waals effects dominate. For Janus TMDs with short rolled length, the curvature induced by intrinsic strain and van der Waals interactions cooperatively leads to bistable morphologies, characterized by scroll and arch conformations. Therefore, Janus nanoscrolls could serve as building blocks for nanoscale mechanically switchable devices.

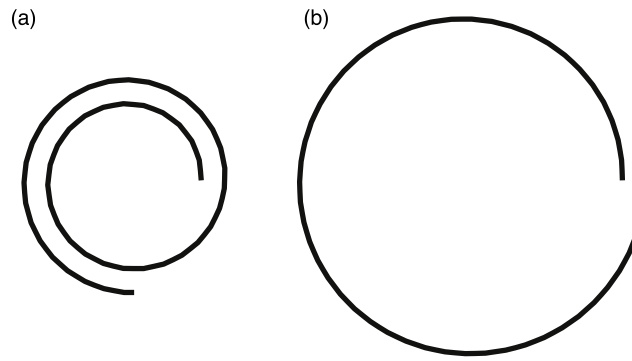


**Fig. 6.** Cross-sectional shape of MoS<sub>2</sub> with (a)  $r_0 = 2$  nm and  $L = 25$  nm at position A in Figs. 4(a) and 4(b)  $r_0 = 4$  nm and  $L = 25$  nm at position B in Fig. 4(a). For simplicity, the atomic positions of Mo atoms are shown.

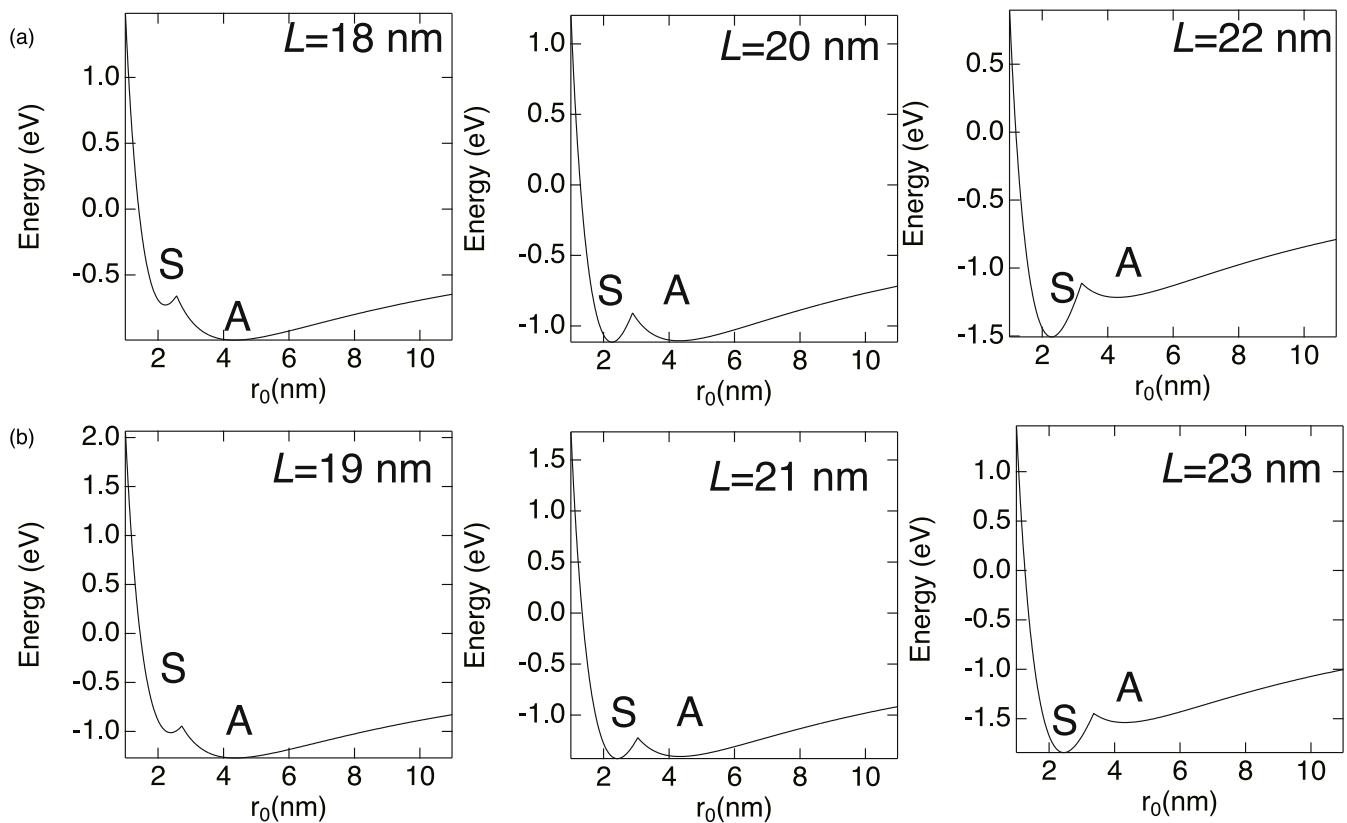


**Fig. 7.** Total energy as a function of inner-most radius  $r_0$  of (a) MoS<sub>2</sub> with  $L = 18, 20$ , and  $22$  nm, and (b) WSe<sub>2</sub> with  $L = 18, 20$ , and  $22$  nm. S and A indicate the scroll and arch conformation, respectively. The energies are measured relative to the flat conformation at each rolled length.

## Acknowledgments

This work was supported by the Japan Science and Technology Agency JST-CREST (Grant Nos. JPMJCR23A4, JPMJCR24A2, and JPMJCR24A5), JST-FOREST (Grant No. JPMJFR213X), the Japan Society for the Promotion of Science JSPS KAKENHI (Grant Nos. JP21H05233, JP21H05234, JP21H05232, JP23H05469, JP25H00417, JP25H00835, JP24H00044, JP22H00280, and JP25K08414), and the Joint Research Program on Zero-Emission Energy Research, Institute of Advanced Energy, Kyoto University.

## ORCID iDs

Yanlin Gao <https://orcid.org/0000-0002-4587-5391>

Mina Maruyama <https://orcid.org/0000-0002-2872-5543>

Yasumitsu Miyata <https://orcid.org/0000-0002-9733-5119>

Susumu Okada <https://orcid.org/0000-0002-0783-3596>

- 1) M. S. Dresselhaus and G. Dresselhaus, *Adv. Phys.* **30**, 139 (1981).
- 2) A. H. Castro Neto, F. Guinea, N. M. R. Peres, K. S. Novoselov, and A. K. Geim, *Rev. Mod. Phys.* **81**, 109 (2009).
- 3) A. K. Geim and I. V. Grigorieva, *Nature* **499**, 419 (2013).
- 4) H. Ago, S. Okada, Y. Miyata, K. Matsuda, M. Koshino, K. Ueno, and K. Nagashio, *Sci. Technol. Adv. Mater.* **23**, 275 (2022).
- 5) S. Iijima, *Nature* **354**, 56 (1991).
- 6) N. Hamada, S.-I. Sawada, and A. Oshiyama, *Phys. Rev. Lett.* **68**, 1579 (1992).
- 7) N. G. Chopra, R. J. Luyken, K. Cherrey, V. H. Crespi, M. L. Cohen, S. G. Louie, and A. Zettl, *Science* **269**, 966 (1995).
- 8) D. Golberg, Y. Bando, M. Eremets, K. Takemura, K. Kurashima, and H. Yusa, *Appl. Phys. Lett.* **69**, 2045 (1996).
- 9) W. Han, Y. Bando, K. Kurashima, and T. Sato, *Appl. Phys. Lett.* **73**, 3085 (1998).
- 10) K. F. Mak, C. Lee, J. Hone, J. Shan, and T. F. Heinz, *Phys. Rev. Lett.* **105**, 136805 (2010).
- 11) A. Splendiani, L. Sun, Y. Zhang, T. Li, J. Kim, C. Y. Chim, G. Galli, and F. Wang, *Nano Lett.* **10**, 1271 (2010).
- 12) R. S. Sundaram, M. Engel, A. Lombardo, R. Krupke, A. C. Ferrari, P. Avouris, and M. Steiner, *Nano Lett.* **13**, 1416 (2013).

© 2026 The Author(s). Published on behalf of

- 13) R. Bacon, *J. Appl. Phys.* **31**, 283 (1960).
- 14) L. M. Viculis, J. J. Mack, and R. B. Kaner, *Science* **299**, 1361 (2003).
- 15) H. Shioyama and T. Akita, *Carbon* **41**, 179 (2003).
- 16) M. Sayyad et al., *Adv. Funct. Mater.* **33**, 2303526 (2023).
- 17) M. Kaneda et al., *ACS Nano* **18**, 2772 (2024).
- 18) Y. Gao, M. Kaneda, T. Endo, H. Nakajo, S. Aoki, T. Kato, Y. Miyata, and S. Okada, *Phys. Rev. B* **110**, 035414 (2024).
- 19) M. Kaneda, W. Zhang, D. Bi, T. Sun, H. Ogura, T. Endo, Y. Takahashi, S. Fujii, T. Kato, and Y. Miyata, *ACS Nano* **19**, 34918 (2025).
- 20) M. Fujita, K. Wakabayashi, K. Nakada, and K. Kusakabe, *J. Phys. Soc. Jpn.* **65**, 1920 (1996).
- 21) K. Nakada, M. Fujita, G. Dresselhaus, and M. S. Dresselhaus, *Phys. Rev. B* **54**, 17954 (1996).
- 22) S. F. Braga, V. R. Coluci, S. B. Legoas, R. Giro, D. S. Galvão, and R. H. Baughman, *Nano Lett.* **4**, 881 (2004).
- 23) Y. Chen, J. Lu, and Z. Gao, *J. Phys. Chem. C* **111**, 1625 (2007).
- 24) T. Li, M. Lin, Y. Huang, and T. Lin, *Phys. Lett. A* **376**, 515 (2012).
- 25) Y. Gao and S. Okada, *Jpn. J. Appl. Phys.* **63**, 085001 (2024).
- 26) Y. Gao and S. Okada, *ACS Appl. Electron. Mater.* **7**, 5861 (2025).
- 27) Y. Miyamoto, S. Saito, and D. Tománek, *Phys. Rev. B* **65**, 041402(R) (2001).
- 28) S. Okada and A. Oshiyama, *Phys. Rev. Lett.* **91**, 216801 (2003).
- 29) S. Okada and T. Kawai, *Jpn. J. Appl. Phys.* **51**, 02BN05 (2012).
- 30) Y. Gao, M. Maruyama, and S. Okada, *Jpn. J. Appl. Phys.* **62**, 015001 (2023).
- 31) S. Okada, S. Saito, and A. Oshiyama, *Phys. Rev. B* **65**, 165410 (2002).
- 32) P. Hohenberg and W. Kohn, *Phys. Rev.* **136**, B864 (1964).
- 33) W. Kohn and L. J. Sham, *Phys. Rev.* **140**, A1133 (1965).
- 34) Y. Morikawa, K. Iwata, and K. Terakura, *Appl. Surf. Sci.* **169**, 11 (2001).
- 35) A simulation tool for atom technology (STATE): <https://state-doc.readthedocs.io/en/latest/index.html>.
- 36) J. P. Perdew, K. Burke, and M. Ernzerhof, *Phys. Rev. Lett.* **77**, 3865 (1997).
- 37) J. P. Perdew, K. Burke, and M. Ernzerhof, *Phys. Rev. Lett.* **78**, 1396 (1997).
- 38) D. Vanderbilt, *Phys. Rev. B* **41**, 7892 (1990).
- 39) Y. Gao and S. Okada, *Appl. Phys. Express* **16**, 075004 (2023).
- 40) T. Shimizu, D. Kamihara, and K. Uchida, *J. Phys. Soc. Jpn.* **92**, 074602 (2023).